J. Chem. Eng. Data 1984, 29, 23–28

Experimental Vapor–Liquid Equilibria in the CO_2–Diethylene Glycol–H_2O and CO_2–Triethylene Glycol–H_2O Systems at Feasible Absorption Temperatures and Pressures

Shinji Takahashi,[†] **Kyoo Y. Song, and Riki Kobayashi***

Department of Chemical Engineering, Rice University, Houston, Texas 77251

The water contents of compressed carbon dioxide gas in equilibrium with diethylene glycol (DEG) solutions of 3.5 and 7.0 wt % water, and with triethylene glycol (TEG) solutions of the same concentrations, have been measured at temperatures of 23.89, 37.78, and 48.89 °C, and pressures of 2.5166, 2.8955, and 5.2745 MPa. A comparison of the dehydration capabilities of the same glycol–water solution for CO_2 with that for natural gas (or methane) indicates that the dehydration qualities for the former (CO_2) exceed those for the latter on an absolute water content basis until a reversal occurs when the CO_2-rich phase begins to assume dense-fluid characteristics. The solubilities of carbon dioxide in the aqueous glycol solutions of the same concentrations and conditions as the water content measurements, and in the pure glycols, are also reported. The CO_2 solubility in TEG and DEG solutions has been analyzed thermodynamically by applying the Krichevsky–Kasarnovsky (KK) equation to both the glycol solutions and the pure glycols. The thermodynamically predicted data agreed with the experimental or smoothed experimental data to better than 2% for both the pure and aqueous solvents at temperatures ranging from 23.89 to 48.89 °C. In the prediction, the experimental data and thermodynamically consistent low-pressure solubility data were used. Data were extrapolated to essentially zero pressure to deduce the isothermal Henry's law constants.

The dehydration processing of CO_2-rich gases may be expected to occur with increasing frequency in (1) the production of CO_2-rich gases from natural reservoirs, (2) the processing of CO_2-rich gases issuing from CO_2-enhanced oil recovery projects, and (3) other CO_2-rich streams appearing in synthetic fuel, petrochemical, and refining processes.

The water content of CO_2 in equilibrium with liquid water has been studied over a wide range of conditions (*1*). However, systematic studies of the phase equilibria of CO_2 with aqueous glycol solutions have not been reported heretofore.

The objective of this study was to provide basic data for the development of the technology to prepare CO_2-rich gases in enhanced oil recovery and the reprocessing of such gases for reinjection into the reservoir.

Experimental Method

The apparatus used to establish equilibrium at high pressures was a vapor recirculation apparatus previously described by Elliot et al. (*2*). The measurement of the water content of the carbon dioxide rich phase utilized (1) sampling lines which were heat-traced and monitored in order to prevent the phase separation of water during its travel from the equilibrium cell to the analytical train, (2) a special analytical method and apparatus developed by Lockwood and McLorie, Inc., based on a patent by Bloch et al. (*3*) designed to analyze water concentrations with good precision down to the sub-ppm range, and (3) a calibrated buret to measure the volumes of the carbon dioxide sample at a fixed, near-ambient temperature. Further details of the analytical procedures are described in a manual distributed by Lockwood and McLorie, Inc.

In essence, the procedure developed by Bloch et al. (*3*), and commercialized by Lockwood and McLorie, Inc., consists of the absorption of water onto a first glycerol column (D in Figure 1) from a known volume of sample gas (in K of Figure 1), the depressurizing desorption of the gas, the measurement and disposition of the desorbed gas from the first glycerol column, the elution of the absorbed water from the first glycerol column using a helium elution stream, splitting of the elution stream containing the water, passage of the two split streams through two parallel differentially packed chromatographic columns (not shown in Figure 1), thence, through a chromatographic detector programmed to produce two equal water peaks of different retention times, with emf's of opposite signs to give a positive and a negative peak and a simultaneous cancellation of the nonaqueous peak. Areas of the resulting chromatographic peaks are determined with a planimeter to obtain the mass of water associated with the known volume of gas sample. The sum of the peak areas is directly related to the number of moles of water by calibration with a known ether–water solution (*4*) synthesized at 1-atm pressure and a fixed near-ambient temperature.

The analytical train describing the analysis of the liquid phase is somewhat simpler, consisting of a trap to measure the amount of glycol–water solution at a fixed near-ambient pressure and temperature associated with a given volume of CO_2.

The system pressure was measured with a 2000 psia Heise gauge with maximum error of ±0.1% of full scale which was calibrated against a dead-weight gauge. A calibrated platinum resistance thermometer was used for the measurement of cell or liquid bath temperature, to an accuracy of better than ±0.1 °F.

Materials

Dry research-grade carbon dioxide was purchased from the Matheson Gas Co. with a stated minimum purity of 99.8 mol %. The carbon dioxide was used without further purification.

"Reagent-grade" diethylene and triethylene glycols were purchased from the Fisher Scientific Co. The minimum stated purities were 99.8 and 99.0 wt %, respectively, with no more than 0.2 wt % water. Distilled water was used to prepare the glycol–water solutions and the water content of the synthesized solution was checked by a commercially available Karl Fischer titration apparatus.

Experimental Results

Concentration of Water in the Carbon Dioxide Rich Phase. The concentration of water in the carbon dioxide rich fluid phase was first plotted as mole fraction of water (log scale) as a

---

[†] Tohoku University, Sendai, Japan.

0021-9568/84/1729-0023$01.50/0

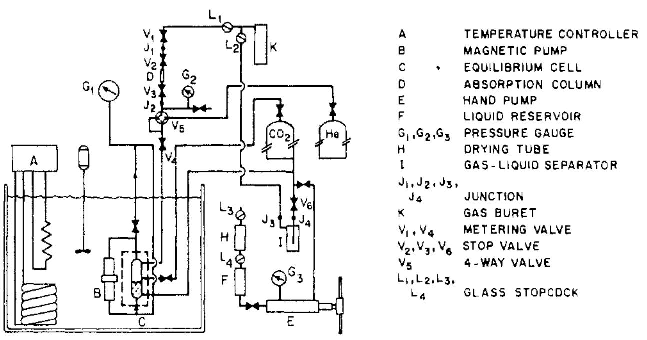

Figure 1. Schematic diagram for recycle vapor-liquid equilibrium apparatus.

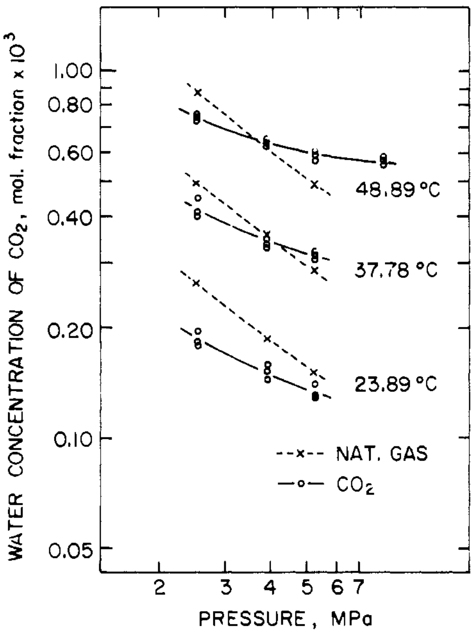

Figure 2. Water concentrations in gaseous CO_2 phase in equilibrium with TEG-3.5 wt % H_2O solution, and in the gaseous phase of natural gas-H_2O system at constant temperatures.

Table I. Summary of Data on Water Content in CO_2 (mg of H_2O/m^3 of CO_2) in Equilibrium with TEG-H_2O Solution[a]

wt % H_2O in solution		3.5	7.0	100.00[b]
mol % H_2O in solution		23.23	38.58	100.00
content at				
23.89 °C,	2.5166 MPa	138.40	281.93	1169.39
	3.8955 MPa	112.93	240.29	1025.22
	5.2745 MPa	99.16	209.85	945.12
37.78 °C,	2.5166 MPa	313.97	621.54	2434.89
	3.8955 MPa	249.90	464.55	1810.15
	5.2745 MPa	235.48	410.09	1601.90
48.89 °C,	2.5166 MPa	554.26	1038.03	4485.32
	3.8955 MPa	474.16	789.74	3203.80
	5.2745 MPa	440.52	676.00	2707.21
	8.0324 MPa	426.11	607.12	2787.31

[a] 1 atm. [b] Reference 1.

function of pressure (log scale) as in Figure 2 for a fixed glycol-water concentration. Multiple samples were taken at each concentration, temperature, and pressure to demonstrate that the successive samples yielded near-reproducible results.

An extraordinarily large number of preliminary runs were conducted before results of the sort presented herein were obtained.

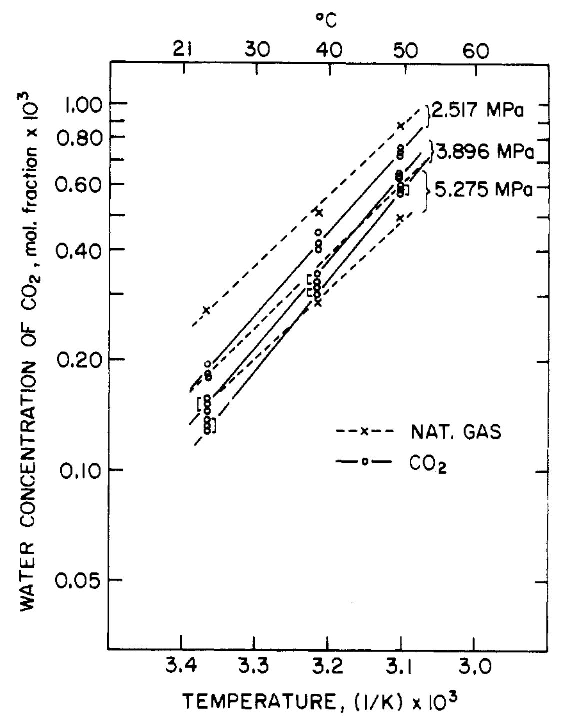

Figure 3. Water concentrations in gaseous CO_2 phase in equilibrium with TEG-3.5 wt % H_2O solution, and in the gaseous phase of natural gas-H_2O system at constant pressures.

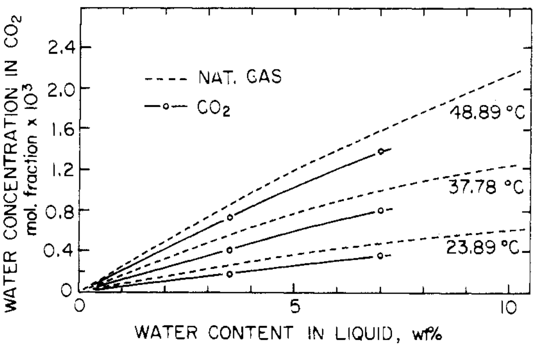

Figure 4. Water concentrations in gaseous CO_2 phase in equilibrium with TEG-water solutions, and in the gaseous phase of natural gas-water system at 2.517 MPa (constant T).

Table II. Summary of Data on Water Content in CO_2 (mg of H_2O/m^3 of CO_2) in Equilibrium with DEG-H_2O Solution[a]

wt % H_2O in solution		3.5	7.0	100.00[b]
mol % H_2O in solution		17.61	30.73	100.00
content at				
23.89 °C,	2.5166 MPa	148.82	293.15	1169.39
	3.8955 MPa	109.41	211.45	1025.22
	5.2745 MPa	98.04	197.03	945.12
37.78 °C,	2.5166 MPa	293.15	504.60	2434.89
	3.8955 MPa	209.85	373.24	1810.15
	5.2745 MPa	184.22	333.20	1601.90
48.89 °C,	2.5166 MPa	472.56	933.91	4485.32
	3.8955 MPa	366.84	626.34	3203.80
	5.2745 MPa	328.39	523.82	2707.21
	8.0324 MPa	286.74	454.94	2787.31

[a] 1 atm. [b] Reference 1.

As the data were being taken, the water concentrations were also plotted as water concentration (log scale) vs. temperature (inverse absolute temperature scale) at a fixed pressure and glycol-water concentrations to divulge the relative consistency of the isobars and the experimental scatter of the data (Figure 3). Data at each pressure and glycol-water concentration were examined with similar plots.

The resulting water concentration data in equilibrium with triethylene glycol-water solutions are presented in Table I and similar data with diethylene glycol-water solutions presented in

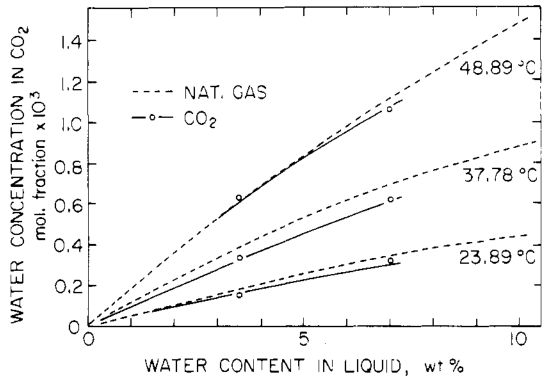

Figure 5. Water concentrations in gaseous CO_2 phase in equilibrium with TEG-water solutions, and in the gaseous phase of natural gas-H_2O system at 3.896 MPa (constant *T*).

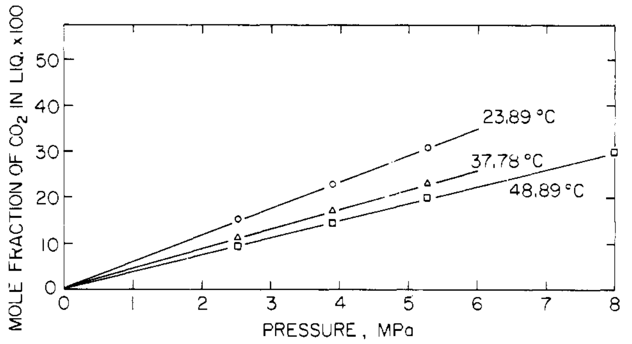

Figure 6. CO_2 solubility in TEG-3.5 wt % H_2O at constant temperatures.

Table II. The data reported represent the arithmetic average of multiple runs, with up to four measurements being taken, for each pressure, temperature, and glycol-water concentration.

While the goal of this investigation was to measure the concentration of water in the carbon dioxide rich phase at relatively low water concentrations in the glycols, an integral view of the data obtained in this study and the terminal water concentration values at zero and 1.0 mole fraction in the liquid phase produced revealing figures similar to Figure 4.

Finally, the water content of carbon dioxide was compared with the water content of carbon dioxide in equilibrium with natural gas or methane as in Figure 5. At moderate absorption pressures, the water concentration of carbon dioxide in equilibrium with the glycol-water solutions was equal to or lower than the water concentration in natural gas at a corresponding pressure, temperature, and glycol-water concentration. In making this comparison the water content chart used was an enlarged version of that presented by Katz et al. (*5*). At higher pressures, however, there appears to be a crossover in the isothermal water concentration vs. pressure curves for carbon dioxide-glycol and methane-glycol solutions as evidenced by Figure 2.

Solubility of Carbon Dioxide in the Liquid Phase. The solubility of carbon dioxide in pure water was measured by Wiebe and Gaddy (*1*, *6*). The solubilities of CO_2 in ethylene and diethylene glycols have been presented up to a total pressure of 20 atm by the Dow Chemical Co. (*7*). In this study measurements have been extended to include the solubility of carbon dioxide in pure diethylene glycol and in pure triethylene glycol at 23.89, 37.78, and 48.89 °C up to pressures as high as 8.0324 MPa (see Tables III and IV). Plots of the original data for the solubility of carbon dioxide in mole percent in TEG-H_2O solution are shown as in Figure 6. Data are also presented in tabular form for the solubility of carbon dioxide in solutions of 23.23 and 38.58 mol % water in triethylene glycol and in 17.61 and 30.73 mol % water in diethylene glycol.

Table III. Summary of CO_2 Solubility Data in TEG-Water Solution[a]

		mL of CO_2/mL of Solution			
wt % H_2O in solution		0.0	3.5	7.0	
mol % H_2O in solution		0.0	23.23	38.58	
solubility at					
23.89 °C,	2.5166 MPa	46.3	40.2	33.3	
	3.8155 MPa	76.4	67.4	56.6	
	5.2745 MPa	113.8	98.2	81.2	
37.78 °C,	2.5166 MPa	31.9	28.3	25.2	
	3.8955 MPa	57.6	46.5	42.1	
	5.2745 MPa	84.9	68.1	58.0	
48.89 °C,	2.5166 MPa	29.8	23.3	23.3	
	3.8955 MPa	48.8	38.1	39.5	
	5.2745 MPa	69.5	56.0	56.4	
	8.0324 MPa	133.7	97.0	88.6	
		mL of CO_2/g of Solution			
wt % H_2O in solution		0.0	3.5	7.0	100.00[b]
mol % H_2O in solution		0.0	23.23	28.58	100.00
solubility at					
23.89 °C,	2.5166 MPa	38.8	33.80	28.1	16.86
	3.8955 MPa	64.1	56.7	47.7	23.76
	5.2745 MPa	95.4	82.6	68.4	28.44
37.78 °C,	2.5177 MPa	26.8	23.8	21.2	12.12
	3.8955 MPa	48.3	39.1	35.5	17.28
	5.2745 MPa	71.2	57.3	48.9	21.23
48.89 °C,	2.5166 MPa	25.0	19.6	19.6	9.70
	3.8955 MPa	40.9	32.0	33.3	14.50
	5.2745 MPa	58.3	47.1	47.5	18.34
	8.0324 MPa	112.1	81.6	68.7	23.20

[a] 1 atm. [b] References *1* and *6*.

Table IV. Summary of CO_2 Solubility Data in DEG-Water Solution[a]

		mL of CO_2/mL of Solution			
wt % H_2O in solution		0.0	3.5	7.0	100.0
mol % H_2O in solution		0.0	17.61	30.73	100.0
solubility at					
23.89 °C,	2.5166 MPa	39.9	34.9	31.8	17.8
	3.8955 MPa	67.5	59.9	52.5	25.1
	5.2745 MPa	106.0	86.8	74.9	30.0
37.78 °C,	2.5166 MPa	31.1	27.3	25.8	12.8
	3.8955 MPa	51.0	42.1	40.0	18.2
	5.2745 MPa	76.5	62.7	60.2	22.4
48.89 °C,	2.5166 MPa	24.8	24.5	20.3	10.2
	3.8955 MPa	41.1	38.2	33.6	15.3
	5.2745 MPa	59.3	53.1	50.9	19.4
	8.0324 MPa	110.5	85.5	80.9	24.5
		mL of CO_2/g of Solution			
wt % H_2O in solution		0.0	3.5	7.0	100.00[b]
mol % H_2O in solution		0.0	17.61	30.73	100.00
solubility at					
23.89 °C,	2.5166 MPa	33.7	29.5	26.9	16.86
	3.8955 MPa	57.0	50.7	44.5	23.76
	5.2745 MPa	89.5	73.5	63.5	28.44
37.78 °C,	2.5166 MPa	26.3	23.1	21.9	12.12
	3.8955 MPa	43.1	35.6	33.9	17.28
	5.2745 MPa	64.6	53.1	51.0	21.23
48.89 °C,	2.5166 MPa	20.9	20.7	17.3	9.70
	3.8955 MPa	34.7	32.3	28.5	14.50
	5.2745 MPa	50.1	44.9	43.1	18.34
	8.0324 MPa	93.3	72.4	68.6	23.20

[a] 1 atm. [b] References *1* and *6*.

Again, we have taken advantage of the available data on the solubility of carbon dioxide (*6*) in pure water and the pure glycol data of this study to present the solubility of carbon dioxide in the solutions over the entire concentration range, albeit we acknowledge the tentativeness of the plots over a considerable range of concentrations. Figure 7 provides an example of the plots obtained. The nonlinear dependence of the solubility on concentration was apparent, particularly at the higher pressures.

Application of Krichevsky-Kasarnovsky Equation in the Prediction of Carbon Dioxide Solubility in Glycol Solutions.

Table V. Experimental and Predicted Solubility of Carbon Dioxide in TEG Solution

T, °F/°C	P, psia/MPa	x_{CO_2} sm exptl	x_{CO_2} pred	x_{CO_2} exptl	$(f^\circ/x)_{CO_2,P=0}$, MPa	$\overline{V}_{CO_2}$, L/g-mol
		TEG-CO_2				
75/23.89	365/2.516	0.205	0.202	0.207	11.95	−0.09023
	435/2.999	0.238	0.239			
	565/3.896	0.301	0.305	0.301		
	725/4.998	0.376	0.379			
	765/5.274	0.395	0.393	0.391		
100/37.78	365/2.516	0.156	0.159	0.153	15.50	−0.0941
	435/2.999	0.186	0.188			
	565/3.896	0.237	0.236	0.245		
	725/4.998	0.305	0.305			
	765/5.274	0.322	0.321	0.324		
120/48.89	365/2.516	0.144	0.138	0.144	18.37	−0.1133
	435/2.999	0.169	0.164			
	565/3.896	0.218	0.214	0.216		
	725/4.998	0.278	0.273			
	765/5.274	0.292	0.288	0.282		
	870/5.998	0.330	0.327			
	1015/6.916	0.378	0.379			
	1165/8.032	0.430	0.432	0.430		
abs av %[b]		1.40		2.06		
		TEG-3.5 wt % Water-CO_2				
75/23.89	365/2.516	0.153	0.153	0.153	16.05	−0.1097
	435/2.999	0.181	0.182			
	565/3.896	0.232	0.234	0.233		
	725/4.998	0.292	0.293			
	765/5.274	0.306	0.304	0.306		
100/37.78	365/2.516	0.113	0.114	0.113	21.77	−0.1042
	435/2.999	0.135	0.136			
	565/3.896	0.174	0.171	0.173		
	725/4.998	0.222	0.222			
	765/5.274	0.235	0.233	0.235		
120/48.89	365/2.516	0.095	0.094	0.095	27.13	−0.1263
	435/2.999	0.112	0.113			
	565/3.896	0.146	0.147	0.146		
	725/4.998	0.190	0.189			
	765/5.274	0.201	0.200	0.201		
	870/4.998	0.226	0.228			
	1015/6.916	0.265	0.266			
	1165/8.032	0.304	0.304	0.304		
abs av %[b]		0.72		0.62		
		TEG-7.0 wt % Water-CO_2				
75/23.89	365/2.516	0.112	0.112	0.111	22.89	−0.1466
	435/2.999	0.135	0.133			
	565/3.896	0.175	0.174	0.175		
	725/4.998	0.223	0.221			
	765/5.274	0.233	0.231	0.233		
100/37.78	365/2.516	0.087	0.088	0.086	28.52	−0.1117
	435/2.999	0.105	0.104			
	565/3.896	0.135	0.132	0.136		
	725/4.998	0.170	0.172			
	765/5.274	0.179	0.181	0.178		
120/48.89	365/2.516	0.080	0.079	0.080	32.48	−0.1302
	435/2.999	0.098	0.095			
	565/3.896	0.129	0.124	0.129		
	725/4.998	0.165	0.160			
	765/5.274	0.174	0.169	0.174		
	870/5.998	0.194	0.192			
	1015/6.916	0.227	0.224			
	1165/8.032	0.255	0.257	0.250		
abs av %	1165/8.032	1.50		2.03		

[a] Smoothed experimental. [b] abs av % = 100[abs(pred − sm exptl or exptl)/pred].

The Krichevsky–Kasarnovsky (KK) equation (*8*) has been successfully applied in the prediction and smoothing of carbon dioxide solubility in propylene carbonate at elevated pressures and higher than ambient temperatures by Mantor et al. (*9*).

The CO_2 solubility is given in Tables III and IV for DEG– and TEG–water solutions of various concentrations and is plotted as mole fraction of carbon dioxide vs. pressure in Figure 6. The low-pressure solubility was estimated from such a plot for each system. For volume conversions and the fugacities of CO_2, ref *10* was consulted.

The Henry's law constants of the KK equation were determined from the junction where P was equal to saturated vapor pressure of the glycol, P_s (essentially negligible), from the plot of $(P - P_s)/(2.303RT)$ vs. $\log (f^\circ/x)_{CO_2}$. The slope of the plot is the partial molar volume of the solute. Again, the isothermal CO_2 solubility in the relatively high pressure region covered in the current investigation has been predicted from the KK equation using the Henry's law constants and partial molar volumes of carbon dioxide determined. The predicted and smoothed experimental data are compared with the experi-

Table VI. Experimental and Predicted Solubility of Carbon Dioxide in DEG Solution

T, °F/°C	P, psia/MPa	x_{CO_2} sm exptl[a]	x_{CO_2} pred	x_{CO_2} exptl	$(f^\circ/x)_{CO_2,P=0}$, MPa	$\overline{V}_{CO_2}$, L/g-mol
		DEG-CO_2				
75/23.89	365/2.516	0.136	0.136	0.138	19.12	−0.1640
	435/2.999	0.163	0.163			
	565/3.896	0.213	0.214	0.213		
	725/4.998	0.273	0.274			
	765/5.274	0.286	0.286	0.286		
100/37.78	365/2.516	0.110	0.109	0.111	24.18	−0.1689
	435/2.999	0.131	0.132			
	565/3.896	0.170	0.169	0.170		
	725/4.998	0.220	0.226			
	765/5.274	0.235	0.240	0.235		
120/48.89	365/2.516	0.091	0.090	0.091	29.24	−0.1534
	435/2.999	0.108	0.108			
	565/3.896	0.141	0.142	0.142		
	725/4.998	0.182	0.185			
	765/5.274	0.193	0.196	0.192		
	870/5.998	0.220	0.225			
	1015/6.916	0.262	0.264			
	1165/8.032	0.308	0.306	0.307		
abs av %[b]		0.81		1.10		
		DEG-3.5 wt % Water-CO_2				
75/23.89	365/2.516	0.107	0.107	0.107	24.30	−0.1665
	435/2.999	0.129	0.128			
	565/3.896	0.170	0.169	0.171		
	725/4.998	0.218	0.217			
	765/5.274	0.230	0.227	0.230		
100/37.78	365/2.516	0.082	0.084	0.086	30.68	−0.1486
	435/2.999	0.098	0.100			
	565/3.896	0.128	0.128	0.126		
	725/4.998	0.168	0.169			
	765/5.274	0.177	0.179	0.177		
120/48.89	365/2.516	0.073	0.073	0.078	35.18	−0.1241
	435/2.999	0.088	0.087			
	565/3.896	0.115	0.113	0.116		
	725/4.998	0.145	0.145			
	765/5.274	0.153	0.154	0.154		
	870/5.998	0.175	0.175			
	1015/6.916	0.205	0.204			
	1165/8.032	0.235	0.233	0.227		
abs av %[b]		0.87		1.97		
		DEG-7.0 wt % Water-CO_2				
75/23.89	365/2.516	0.087	0.086	0.087	31.21	−0.1892
	435/2.999	0.103	0.103			
	565/3.896	0.136	0.136	0.136		
	725/4.998	0.175	0.177			
	765/5.274	0.186	0.185	0.184		
100/37.78	365/2.516	0.068	0.068	0.072	39.67	−0.1923
	435/2.999	0.082	0.082			
	565/3.896	0.109	0.107	0.107		
	725/4.998	0.143	0.144			
	765/5.274	0.153	0.153	0.153		
120/48.89	365/2.516	0.058	0.058	0.057	45.86	−0.1584
	435/2.999	0.069	0.069			
	565/3.896	0.093	0.091	0.092		
	725/4.998	0.121	0.119			
	765/5.274	0.128	0.126	0.133		
	870/5.998	0.146	0.145			
	1015/6.916	0.170	0.171			
	1165/8.032	0.196	0.198	0.195		
abs av %		0.84		1.75		

[a] Smoothed experimental. [b] abs av % = 100[abs(pred − sm exptl or exptl)/pred].

mental values in Tables V and VI showing an absolute average deviation of less than 2% in every system investigated.

Discussion

The water content of the CO_2 in equilibrium with DEG– and TEG–water solutions indicates that over a wide range of conditions the latter dehydrates CO_2 more effectively than natural gases at the same pressure, temperature, and glycol concentration. However, as the pressures approach values wherein CO_2 begins to assume dense-fluid behavior, the relative dehydration effectiveness is reversed.

The extraordinary ability of the glycols to dehydrate CO_2-rich gases is attributed to the high solubility of CO_2 in the solvent phase, a characteristic presently being investigated.

Since the CO_2 is so soluble in the glycol–water solution, calorimetric measurements of the heat of solution of CO_2 in the glycols should be determined.

The data measured in this report have been combined with measurements reported in the literature, by Wiebe and Gaddy

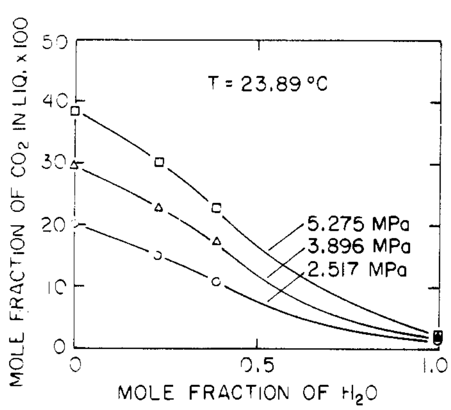

Figure 7. CO_2 solubility in TEG–H_2O solution at 23.89 °C and constant pressures.

(*1*, *6*), to present dehydration and solubility data from 100% glycol to pure water at various temperatures, pressures, and concentrations in Tables I–IV.

The Krichevsky–Kasarnovsky equation has been successfully utilized in the prediction of the carbon dioxide solubility values in aqueous solutions of DEG and TEG and in pure DEG and pure TEG just as in propylene carbonate (*9*).

Acknowledgment

We acknowledge the role of the Arco Oil and Gas Co. for the support of this work both monetarily and technically during the course of the work. Mr. Raymond J. Martin contributed to the modification and maintenance of the apparatus throughout the course of the study.

Registry No. Carbon dioxide, 124-38-9; diethylene glycol, 111-46-6; triethylene glycol, 112-27-6.

Literature Cited

(1) Wiebe, R.; Gaddy, V. L. *J. Am. Chem. Soc.* **1941**, *63*, 475.
(2) Elliot, D. G.; Chen, R. J.; Chappelear, P. S.; Kobayashi, R. *J. Chem. Eng. Data* **1974**, *19*, 71.
(3) Bloch, M. G.; Lifland P. P. U.S. Patent 3 405 550, 1968.
(4) "International Critical Tables, National Research Council"; McGraw-Hill: New York, 1928; Vol. III, p 388.
(5) Katz, D. L.; Cornell, D.; Kobayashi, R.; Poettmann, F. H.; Vary, J. A.; Elenbaas, J. R.; Weinaug, C. F. "Handbook of Natural Gas Engineering"; McGraw-Hill: New York, 1959; Chapter 5.
(6) Wiebe, R.; Gaddy, V. L. *J. Am. Chem. Soc.* **1940**, *62*, 815.
(7) "Gas Conditioning Fact Book"; Dow Chemical Co.: Midland, MI, 1962.
(8) Krichevsky, I. R.; Kasarnovsky, J. S. *J. Am. Chem. Soc.* **1935**, *57*, 2168.
(9) Mantor, P. D.; Abib, O., Jr.; Song, K. Y.; Kobayashi, R. *J. Chem. Eng. Data* **1982**, *27*, 243-5.
(10) Altunin, V. V.; Gadetskii, O. G.; Chapela, G. A.; Rowlinson, J. S. "IUPAC International Thermodynamic Tables of the Fluid State, Carbon Dioxide"; Angus, S., Armstrong, B., Eds.; Pergamon Press: Oxford, England, 1976.

Received for review December 13, 1982. Revised manuscript received June 13, 1983. Accepted June 23, 1983. Arco Oil and Gas Co. provided financial support for this work.

Isobaric Vapor–Liquid Equilibria of the Tetrahydrofuran/Ethanol System at 25, 50, and 100 kPa

Erwin Brunner* and Andreas G. R. Scholz

BASF Aktiengesellschaft, D-6700 Ludwigshafen/Rhein, Federal Republic of Germany

The vapor–liquid equilibrium of the system tetrahydrofuran (THF)/ethanol at 25, 50, and 100 kPa has been determined experimentally by using an equilibrium still of the recirculation type. Data reduction based on the Wilson, NRTL, and UNIQUAC models provides a correlation for γ_i. The tetrahydrofuran/ethanol system forms an azeotrope above 53 kPa. At 100 and 150 kPa, the azeotropic mixtures contain respectively 0.908 and 0.844 mole fraction of tetrahydrofuran.

Introduction

In the present investigation the vapor–liquid equilibrium of the tetrahydrofuran (THF)/ethanol system was measured because there are only conflicting data in the literature for this system. Horsley (*1*) lists an azeotropic point of 0.85 mole fraction THF at atmospheric pressure. From boiling point measurements alone, Yoshikawa, Takagi, and Kato (*2*) have derived an azeotropic point at 0.905 mole fraction THF at 65.7 °C at atmospheric pressure. In contrast, Bernshtein, Generalova, Zelvenskii, and Shalygin (*3*), although employing a refined technique of radiometric analysis (radioactive ethanol with ^{14}C), did not find an azeotrope at atmospheric pressure when the ethanol content is low. In order to clarify these conflicting results, we measured the vapor–liquid equilibrium at 25, 50, and 100 kPa and furthermore the compositions of the azeotrope at 100, 125, and 150 kPa were determined by using a packed column.

Experimental Section

Purity of the Components. The reagents, manufactured by BASF Aktiengesellschaft, Federal Republic of Germany, were used without further purification. Their purity was confirmed by gas chromatography and Karl Fischer titration: tetrahydrofuran, >99.9%; ethanol, >99.9% (water content 0.03).

Apparatus and Procedure. The still used to obtain vapor–liquid equilibrium data was a Hunsmann vapor–liquid recirculation still (*4*), with several modifications suggested by Brunner and Scholz (*5*) and comprising, in the main, an improved protective screen against heat losses, an intensive stirrer for the liquid phase, a nonreturn valve in the condensate return, and simpler sampling of the vapor phase.

With the all-glass equilibrium still, which is shown in Figure 1, equilibrium measurements may be made in the range from 2 to 150 kPa.

Because four Cottrell tubes are employed and a very small volume of condensate (about 2 cm^3) is present, the vapor–liquid equilibrium is established in only 10–15 min. The liquid space in the apparatus is filled so that, when the liquid boils, a continuous stream of vapor–liquid mixture passes through the four Cottrell tubes and bathes the platinum resistance thermometer. In the thermometer space, the liquid and the vapor, which are in equilibrium with each another, are separated. The vapor is

0021-9568/84/1729-0028$01.50/0